Russian Chemical Bulletin, International Edition, Vol. 60, No. 6, pp. 1071—1077, June, 2011

The role of the medium in electrochemical functionalization and dispersion of carbon nanotubes

A. G. Krivenko,[a★] ***N. S. Komarova,***[a] ***A. G. Ryabenko,***[a] ***A. V. Naumkin,***[b] ***E. V. Stenina,***[c]
L. N. Sviridova,[c] ***and S. N. Sul´yanov***[d]

[a]*Institite of Problems of Chemical Physics, Russian Academy of Sciences,*
1 prosp. Akad. Semenova, 142432 Chernogolovka, Moscow Region, Russian Federation.
Fax: +7 (496) 522 3507. E-mail: krivenko@icp.ac.ru
[b]*A. N. Nesmeyanov Institute of Organoelement Compounds, Russian Academy of Sciences,*
28 ul. Vavilova, 119991 Moscow, Russian Federation.
Fax: +7 (499) 135 5328
[c]*Department of Chemistry, M. V. Lomonosov Moscow State University,*
3 Bidg. 1, Leninskie Gory, 119992 Moscow, Russian Federation.
Fax: +7 (499) 939 0067
[d]*A. V. Shubnikov Institute of Crystallography, Russian Academy of Sciences,*
59 Leninsky prosp., 119333 Moscow, Russian Federation.
Fax: +7 (499) 135 1011

An electrochemical method for dispersion of single-walled carbon nanotubes (SWNTs) is described. The technique is based on grafting of oxygen-containing functional groups to the nanotube surface during electrolysis in aqueous and nonaqueous potassium bromide solutions. A dependence of the degree of functionalization of nanotubes on the solvent was revealed experimentally. Nanotubes treated in DMSO have about 14 carbon atoms per oxygen atom from functional groups (*cf.* nearly four C atoms per oxygen atom in the nanotubes treated in aqueous solutions). The corresponding maximum specific capacities of the electrodes are nearly 10 and 60 F g^{-1}. The samples treated in solutions of KBr in DMSO have about 300 carbon atoms per bromine atom on the nanotube surface (*cf.* only 30 carbon atoms in the samples treated in aqueous solution). A mechanism of electrochemical modification of SWNTs is proposed. Its key step is production of atomic oxygen that oxidizes the nanotube surface with the formation of functional groups.

Key words: single-walled carbon nanotubes, dispersion, functionalization, electrolysis, dimethylsulfoxide.

At present, there are only a few fields of application of nanosized carbon and, in particular, carbon nanotubes. For instance, nanotubes can be used as components of polymer-nanotube composites.[1] Indeed, the introduction of very small amounts (~10^{-3}—10^{-2} wt.%) of single-walled carbon nanotubes (SWNTs) into a polymer matrix leads to a noticeable improvement of operational efficiency of such composites.[2] However, an increase in the SWNT concentration to about 1—5 wt.% usually causes the strength of a material to decrease.[3] It is believed that such a behavior is due to sliding motion of nanotubes relative to one another in nanotube bundles formed at sufficiently high concentration of SWNTs in the initial monomer. This sliding motion causes nanotubes to split off from the polymeric material.[4] Therefore, the design of high-strength, nanotube-based composites requires individualization of nanotubes followed by their dispersion in the polymer matrix. Also, the number of functional groups covalently bound to the nanotube surface should be optimal. A particular number of functional groups is necessary to form strong bonds between the individual SWNT and the polymer matrix, but if the number of such bonds is too large, the properties of the nanotube deteriorate.

Both these problems, *viz.*, dispersion and controlled functionalization of nanotubes, are far from being solved. There are neither commonly accepted method for the synthesis of particular types of individual nanotubes nor relevant procedures for their purification.[5] Usually, the available nanotube preparations represent mixtures of carbon nanotubes with different diameters, lengths, and chiralities. Moreover, they often contain uncontrolled amounts of metallic and graphitic impurities. In addition, nanotubes can form, through van der Waals forces, either hexagonally packed bundles typical of "short" SWNT with an

Published in Russian in *Izvestiya Akademii Nauk. Seriya Khimicheskaya,* No. 6, pp. 1046—1052, June, 2011.

average length of 1 μm or coils of "long" nanotubes with average length ranging from 10 to 1000 μm. The energy of van der Waals interaction between individual SWNTs is 0.5—1.0 eV per nanometer.[6] Such a strong interaction is the major obstacle to dispersion of individual SWNTs in aqueous and organic solutions and polymer matrices.

Unfortunately, considerable literature on methods for functionalization and dispersion of SWNTs includes only few studies concerning electrochemical approaches and methods. In particular, electrochemical disruption of nanotube bundles (without oxidation of the surface) by incorporating Li ions solvated by DMSO molecules into channels between tubes was reported.[7] However, the electrolyte decomposes at the potentials used by the authors of Ref. 7. This precludes complete individualization of nanotube from bundles. There is also an electrochemical method for partial disruption of nanotubes during electrolysis of aqueous chloride solutions.[8] Some chlorine atoms produced in the course of electrolysis at a specified potential move into the voids between tubes and adsorb on the surface of nanotubes as well as form covalent bonds with nanotube carbon atoms. Other Cl atoms interact with water with the formation of hypochlorite ions which decompose and thus serve as sources of atomic oxygen that causes the oxidation of the nanotube surface and the formation of various covalent bonds. In this work, we compare the effect of electrolysis of KBr solutions on the dispersion and functionalization of SWNTs in aqueous and nonaqueous (DMSO) solutions. Potassium bromide was chosen as the background electrolyte because it is well soluble in aqueous and nonaqueous electrolytes and bromine ions have a low oxidation potential; DMSO is a readily available aprotic solvent of relatively low toxicity. Owing to easy penetration through the skin of a living organism,[9] it is widely used in biology and medicine as drug delivery agent. One can assume that the use of DMSO as organic solvent for dispersion of SWNT bundles will make it possible to extend the field of application of individual nanotubes in medicine. In addition, the authors of some studies reported the efficiency of DMSO as a solvent for functionalized nanotubes[10,11] and high wettability of carbon nanotubes in DMSO.[12]

Experimental

Electrochemical studies were carried out by cyclic voltammetry (CV) using an IPC-Pro L potentiostat. Aqueous solutions were prepared using water triple distilled in quartz vessels. DMSO was stored over alkali and distilled *in vacuo*. From ^{1}H NMR spectra recorded on a Brucker Nova 500 spectrometer operating at 500 MHz it follows that the concentration of water in DMSO solutions was at most 0.22 mol.% while the concentration of the main substance was 99.7%. Prior to measurements, the dissolved oxygen was removed by bubbling argon (high purity grade) over a period of about 40 min. The salts of extra pure grade were used as is. All potentials (*E*) are given relative to aqueous saturated calomel electrode.

Single-walled carbon nanotubes for the preparation of nanopaper were synthesized by the electric arc method using a Ni/Y catalyst. Nanopaper represented a black thin layer of a paper-like material 0.03—0.04 mm thick with a specific surface weight of 1—2 mg cm^{-2} containing 98—99% of nanotubes and less than 0.5% of metal. According to electron microscopy data, nanopaper represents ribbons comprising 500—10000 SWNTs with an average diameter of about 1.4 nm and an average length of nearly 1 μm. In turn, these ribbon form larger carpet-like aggregates up to a few micrometres in size. Carbon nanotubes used in this study were extensively characterized by electron microscopy, IR, NMR spectroscopy, X-ray photoelectron spectroscopy (XPS), and Raman spectroscopy, as well as by mass spectrometry and elemental analysis.[13] The preparation of electrodes based on carbon nanopaper was described earlier.[14]

The content of carbon, oxygen, and nitrogen was determined with an Elementar Vario cube automated CHNS/O analyzer. To determine bromine, the sample was combusted in oxygen in a Schoeninger flask followed by titrimetric determination of Br$^-$ ions. Products of electrolysis of potassium bromide solutions were analyzed using a Shimadzu LC-2020 liquid chromato-mass spectrometer. Thermogravimetric and differential thermal analysis were done with a NETZSCH STA-409 Luxx thermal analyzer with a mass spectrometric accessory for analysis of exhaust gases.

Structural features of SWNTs were studied with a Carl Zeiss LEO 912 AB OMEGA transmission electron microscope using samples prepared by dispersion of nanopaper in isopropyl alcohol under sonication. The UV, visible, and near-IR absorption spectra were recorded using a Lumex FT-02 IR Fourier spectrometer (Lumex Instruments Ltd., Russia). The Raman spectra were acquired with a Thermo Scientific Nicolet 9810 Raman Fourier spectrometer using a laser operating at $\lambda = 976$ nm as the excitation source. The Auger spectra and X-ray photoelectron spectra were recorded with a MK II VG Scientific spectrometer.

Results and Discussion

Passage of electric current through the interface between the solution and the electrode made of nanotube bundles is accompanied by the formation of reactive intermediates (radicals or radical ions) on the surface of SWNTs and near it. These species participate in subsequent homogeneous and heterogeneous reactions resulting in stable molecules or ions. Both intermediates and stable species can penetrate into cavities and channels between SWNTs that form nanotube bundles through van der Waals interaction. One can assume that the molecules and ions are then physically sorbed and chemisorbed on the surface of nanotubes. It is also probable that the most reactive intermediates form covalent bonds with the surface of nanotubes.[8]

In 1.0 *M* aqueous KBr solutions at potentials $E \approx \approx (1—1.5)$ V on the nanopaper electrode, one deals with electrochemical oxidation of bromine ions. According to chromato-mass spectroscopic analysis in solution, the

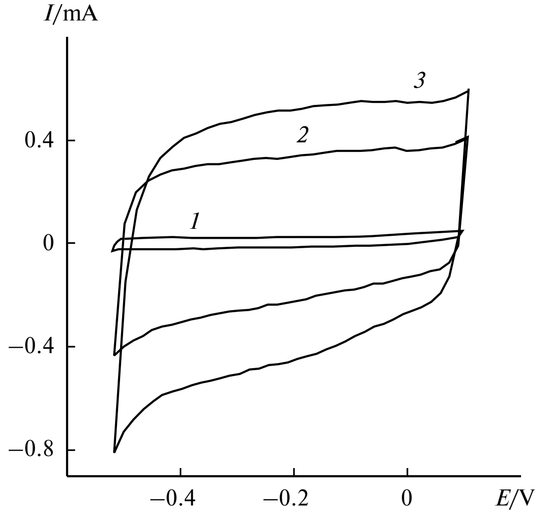

Fig. 1. Cyclic voltammograms of nanotube electrode in 1 *M* aqueous KBr solutions at a potential sweep rate of 0.05 V s^{-1}: initial sample (*1*) and samples electrolyzed for 25 (*2*) and 50 min (*3*). For clarity, the currents of the initial sample are magnified (×4).

major products of the reaction include molecular bromine and Br_2^- ions. The process is accompanied by considerable changes in the CV currents for this electrode in the potential range from 0.1 to −0.5 V (Fig. 1). The absolute values of the forward and reverse potential sweep currents significantly increase, whereas the shapes of the CV curves change only slightly. This corresponds to domination of the charging currents of the double electrical layer over the electrode reaction currents and makes it possible to evaluate the electrical capacity of the samples (C) from a simple ratio $C = I_c/v$, where I_c is the charging current and v is the sweep rate of the potential E. In the course of electrolysis, the initial capacity of electrodes increases 12—50 times, reaches a maximum value after nearly 60 min, and then decreases. The increase in C is apparently due to an increase in the surface area of the SWNT-electrode accessible to the electrolyte solution, while the decrease in the capacity on long-term electrochemical treatment seems to be due to violation of its continuity. This conclusion was also confirmed by transmission electron microscopy data, *viz.*, nanotube bundles in the electrochemically treated samples are disrupted to smaller systems whose width is 5—10 times smaller than that of the initial nanopaper bundles (see Fig. 2, *a*, *b*). Figure 2, *c* also shows no distortion of the SWNT structure upon electrochemical treatment. Figure 3 presents the small-angle X-ray scattering (SAXS) patterns for the initial nanopaper samples and for the nanopaper samples electrochemically treated in aqueous KBr solutions. The X-ray diffraction patterns were recorded at different times of electrochemical treatment. The intensity of the first reflection corresponding to the average distance between tubes in nanotube bundles significantly decreases during electrolysis. Nanotube bundles form a two-dimensional hexagonal lattice whose section is shown in the inset in Fig. 3. Electrochemical treatment of nanopaper causes the distances between tubes to increase randomly; as a consequence, the interplanar spacings are no longer constant and the reflection amplitude decreases. This suggests that electrochemical treatment leads to a greater disordering in the arrangement of nanotubes in the bundles. Figure 4 presents the UV, visible, and near-IR absorption spectra of the initial and electrochemically treated nanotubes. Initial SWNTs have a pronounced van Hove spectrum; however, the band intensities decrease as the time of electrochemical treatment of the samples increases. In particular, the band intensities are halved during the treatment time necessary to achieve a maximum electrical capacity C. This indicates partial violation of the electronic structure of nanotubes, which may probably be due to the appearance of functional groups on their surfaces. Thus, analysis of the absorption spectra confirms the conclusion drawn after comparison of the micrographs

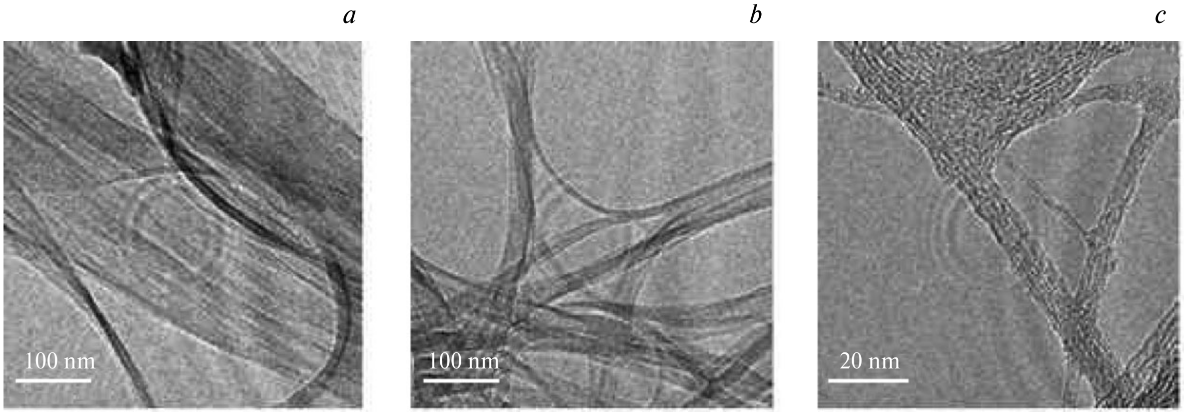

Fig. 2. Micrographs of nanotube bundles in the SWNT sample before (*a*) and after electrochemical treatment in 1 *M* aqueous KBr solution during 50 min (*b*, *c*).

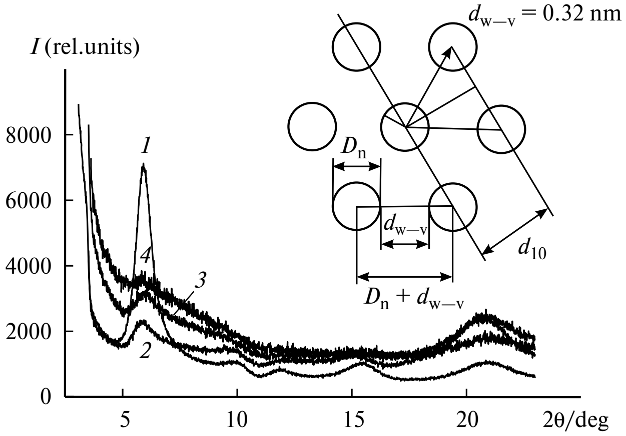

Fig. 3. Small-angle X-ray scattering patterns of the samples of initial nanopaper (*1*) and nanopaper electrochemically treated in 1 *M* aqueous KBr solutions during 15 (*2*), 30 (*3*), and 60 min (*4*). For clarity, the intensities in the SAXS patterns 2—4 are magnified (×2, ×3, and ×5, respectively). Inset: a schematic view of a SWNT bundle; d_{w-v} is the van der Waals inter-tube distance, D_n is the nanotube diameter, and d_{10} is the lattice constant corresponding to the first SAXS reflection (2θ ≈ 6°).

of the SWNT samples (see Fig. 2) that the nanotubes retain their structure until the electrode capacity increases. The results obtained cast some doubt on the statement that weakening of the first reflection in the X-ray diffraction patterns of SWNT is due to breakdown of electrochemically treated nanotubes and to formation of amorphous phase.

Electrolysis in 0.2 *M* solutions of KBr in DMSO at anode potentials $E \approx 0.8—0.9$ V on the nanotube electrode is also accompanied by release of bromine. However, unlike aqueous solutions, the use of higher positive potentials is impossible because of decomposition of the electrolyte at $E \geq 1.0$ V. This decomposition is accompanied by the appearance of specific smell and darkening of the solution. Analysis of the ^{13}C NMR spectra recorded before and after electrolysis revealed no signals corresponding to the DMSO decomposition products at the potentials applied.

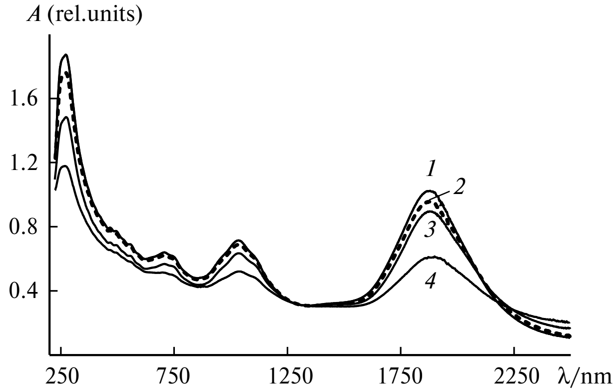

Fig. 4. Absorption spectra of initial SWNTs (*1*) and SWNTs electrochemically treated in 0.2 *M* solution of KBr in DMSO until the maximum electrical capacity (*2*), in 1 *M* aqueous KBr solution for 5 min (*3*), and until the maximum capacity (*4*). All absorption spectra are matched at a wavelength of 1319 nm.

As in aqueous solutions, electrolysis in solutions of KBr in DMSO is accompanied by changes in the shape of the CV curves of the SWNT electrode. However, the initial capacity of the electrode immersed into the DMSO solution is three—four times higher than that of the electrode immersed into aqueous solution (Table 1). Apparently, the working surface area of nanotubes in the electrolyte solution in the nonaqueous medium is larger than in the aqueous solution. It seems that nanotubes are characterized by better wettability in DMSO than in water and therefore the electrolyte (DMSO) can penetrate faster into channels between individual nanotubes in the bundle. In this case, the initial electrode capacity is nearly doubled during electrolysis in the solution of KBr in DMSO, which is much smaller than in aqueous KBr solutions. Long-term electrolysis in the solution of KBr in DMSO causes the capacity *C* to decrease, but the decrease is observed at longer electrolysis times (~80 min) compared to aqueous solutions. Electrochemical treatment in the solutions of KBr in DMSO over a period of 80 min leads to a small (~5%) decrease in the intensity of the van Hove band (see Fig. 4). As in the case of electrolysis in aqueous KBr solutions, this decrease can be associated with violation of the electronic structure of nanotubes, which may be due to the formation of functional groups on their surface. An analysis of the ^{1}H NMR spectra of the electrolyte suggests that the concentration of water in the DMSO solutions (≤0.22 mol.%) remains unchanged during electrolysis. At the same time, assuming that transformation of one H_2O molecule requires one electron, it appears that the charge consumed during electrolysis is more than ten times higher than the number of electrons required for total transformation of all water molecules present in the solution. The fact that water molecules are not involved in electrolysis is

Table 1. Changes in the capacity of nanopaper electrodes during electrochemical treatment in different solvents

Treatment time /min	Capacity/F g^{-1}	
	H_2O, 1 *M* KBr	DMSO, 0.2 *M* KBr
0	1—2	4—5
15	10—12	6—7
30	22—26	7—8
45	58—68	10—12
60	60—68	12—15
75	45—50	14—16
90	—	11—12

probably due to the bulk properties of DMSO. The bulk properties of pure DMSO and its aqueous solutions have been well documented.[15—17] These systems are characterized by self-association and association which are favored by high polarity of the DMSO molecule (μ = 3.96 D) whose positive effective charge (+0.5) is localized on the sulfur atom. Owing to the dipole-dipole interaction and hydrogen bonds, chain and cyclic aggregates exist in liquid DMSO. These aggregates are responsible for the ordered structure of liquid DMSO at $T < 40$ °C. Owing to protophilic properties of DMSO, associates readily break down upon the addition of proton donors. Mixing DMSO with water is a highly exothermic process. The structure characteristic of pure DMSO breaks down and a new structure is formed, which includes hydrogen-bonded water molecules. The highly hydrophilic S=O group can even form bonds with two water molecules. It seems not improbable that water molecules involved in such bonds are much less reactive than in water and therefore do not participate in functionalization of nanotubes in the DMSO solutions.

In an attempt to establish the mechanism of electrochemical action on the SWNT surface during electrolysis of KBr solutions it is of interest to reveal how the solvent nature affects the elemental composition and the state of the nanotube surface. Once the maximum capacity during electrolysis in aqueous solution was reached, the electrode material was analyzed for Br, C, O, and N and the results obtained were compared with the composition of the initial nanopaper (Table 2). From the data of Table 2 it follows that electrochemical treatment leads to an increase in the content of bromine and oxygen in the samples. To establish the nature of the interaction of bromine with the nanotube surface, a treated sample was washed with water and heated to 50—60 °C. Then, thermogravimetric analysis was carried out and the mass spectra of the gases liberated were recorded. It was found that in these samples, the content of bromine chemically bound to nanotube carbon atoms is low. This conclusion is confirmed by the structure of the X-ray photoelectron spectrum of the treated sample which shows a peak at 70.2 eV characteristic of the C—Br bond. From analysis of the C1s peak in the XPS spectra it follows that electrochemical treatment in DMSO does not bring about significant changes in the spectrum, whereas a similar process in aqueous solutions leads to pronounced spectral changes in the high-energy region. This can probably be due to the formation of C—O—C, C=O, and C(O)O bonds. In addition, XPS spectra in the O1s region for all samples are almost the same (Fig. 5, *a*). This suggests that oxygen atoms in these samples are in the same chemical state, although are present in different concentration. The results of quantitative analysis for carbon, oxygen, nitrogen, and bromine on the surface of nanopaper (see Table 2) correlate with the changes in the intensity ratio of the D/G modes in the Raman spectra of nanotubes during electrolysis. This ratio increases to nearly 30.0% after electrochemical treatment in aqueous KBr solution for 60 min (*cf.* about 8.0% for DMSO solution). Taking into account the fact that in the initial sample this ratio was at most 5.1%, one can suggest that the number of defects formed on the SWNT surface during electrolysis in aqueous KBr solutions is much larger than in the DMSO solutions. According to XPS data, there are about 14 carbon atoms per oxygen atom from functional groups after treatment in DMSO (*cf.* nearly 4 carbon atoms after treatment of nanopaper in aqueous solutions). The corresponding maximum specific electrode capacitances are ~15 and ~70 F g^{-1}. The samples treated in the solutions of KBr in DMSO are characterized by a value of about 300 carbon atoms per bromine atom on the nanotube surface (*cf.* only

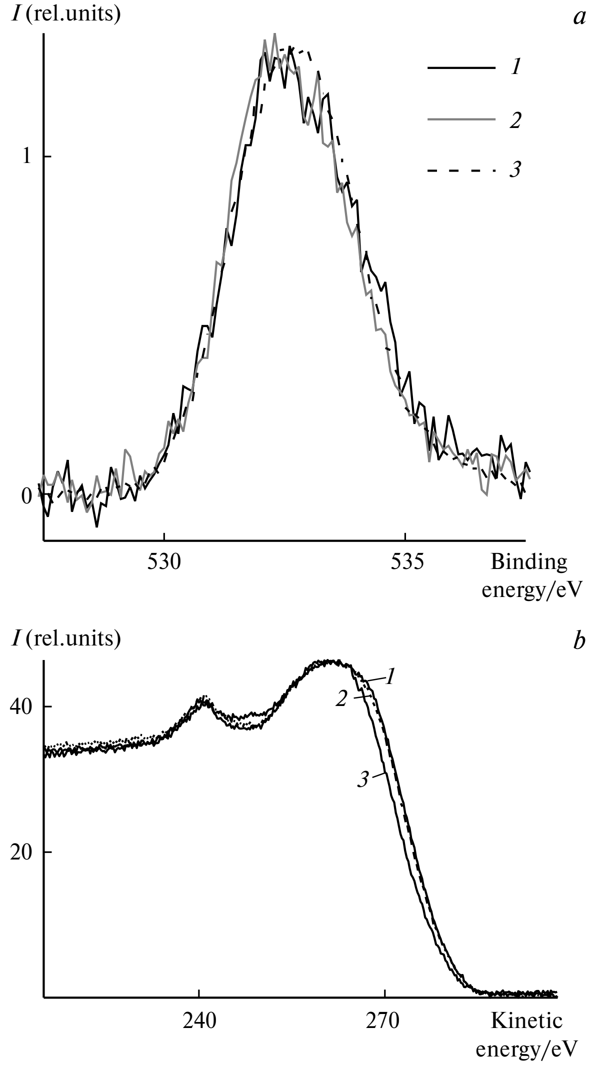

Fig. 5. X-ray photoelectron spectra in the O1s region (*a*) and the lineshape of the C KVV Auger spectra (*b*) of initial SWNTs (*1*) and SWNT samples after electrochemical treatment in 0.2 *M* solution of KBr in DMSO (*2*) and in 1 *M* aqueous KBr solution (*3*). The spectra were normalized to the most intense peak.

Table 2. Results of quantitative XPS analysis of initial nanopaper and nanopaper electrochemically treated in different media*

SWNTs	C1s	O1s	N1s	Br3d
	at.%			
Initial sample	95.0	5.0 [1.0]	0.0 [0.1]	0.0 [0.8]
After electrolysis in 0.2 *M* solution of KBr in DMSO	91.6	6.6	1.0	0.3
After electrolysis in 1 *M* aqueous KBr solution	77.7	18.7 [8.0]	1.0 [0.7]	2.6 [1.3]

*Results of elemental analysis are given in square brackets.

30 carbon atoms for the samples treated in aqueous KBr solution).

Figure 5, *b* presents the Auger spectra of the initial and treated samples of the nanopaper electrodes. It follows that, as for the X-ray photoelectron spectra, the most significant changes are observed in the spectra of the SWNT samples obtained by electrochemical treatment in aqueous KBr solutions. Earlier,[18] it was shown that the shift of the spectra toward lower energies of Auger electrons indicates some changes in the π-band of the density of states in region near the Fermi level. This can be due to both weakening of the inter-tube interaction and oxidation of the sample. A possible oxidation is confirmed by the fact that electrolysis in aqueous KBr solution is accompanied by considerable dispersion of nanotubes and formation of oxygen-containing functional groups on the nanotube surface.

Analysis of the results obtained during electrolysis of aqueous and nonaqueous potassium bromide solutions using a nanostructured carbon electrode as anode suggests a key role of water in the functionalization and dispersion of nanotubes. Relevant mechanisms of these processes are shown in Scheme 1. In the first step, the oxidation of Br^- ion at the electrode results in bromine atom as a reactive intermediate (1) which can react in different manner. The main route includes a reaction with water resulting in hypobromite ion (2). Yet another route implies a direct interaction of bromine atom with the graphene surface of nanotube (3); in addition, bimolecular deactivation (4) is possible. Ignoring the amount of oxygen in the initial samples, the data listed in Table 2 can be used to estimate the lower bound of the ratio of efficiencies of the main and side reaction routes of Br atom. It appears that, in the presence of both solvents, the main reaction route is five to seven times more probable than the side routes.

Reactions included in the main route result in disproportionation of some hypobromite ions to bromate ions (5) detected in solution by chromato-mass spectrometry. Other hypobromite and bromate ions decompose with the formation of atomic oxygen which oxidizes the nanotube surface with the formation of functional groups (6) that impart hydrophilic properties to nanotubes. The affinity of water molecules to nanotube surface becomes higher than the force of the interaction between tubes; this finally leads to disruption of SWNT bundles. Summing up, the main route of functionalization under the electrolysis of bromine ions is the oxidation of SWNT surface rather than halogenation. By choosing the electrolysis medium one can vary the ratio of the degree of functionalization to the degree of dispersion of SWNTs.

Scheme 1

$$Br^- \xrightarrow{\bar{e}} Br \qquad (1)$$

$$2\,Br + H_2O \longrightarrow BrO^- + Br^- + 2\,H^+ \qquad (2)$$

$$Br + SWNT \longrightarrow SWNT\text{-}Br \qquad (3)$$

$$Br + Br \longrightarrow Br_2 \qquad (4)$$

$$BrO^- \xrightarrow{2\,BrO^-} BrO_3{}^- + 2\,Br^- \qquad (5)$$

$$\left.\begin{array}{l} BrO^- \longrightarrow Br^- + [O] \\ BrO^-{}_3 \longrightarrow Br^- + O_2 + [O] \end{array}\right] \xrightarrow{SWNT} SWNT_{ox} \qquad (6)$$

$SWNT_{ox}$ is oxidized SWNT.

References

1. B. S. Banerjee, T. Hemraj-Benny, *Adv. Mater.*, 2005, **17**, 17.
2. E. R. Badamshina, M. P. Gafurova, Ya. I. Estrin, *Usp. Khim.*, 2010, **79**, 1027 [*Russ. Chem. Rev.* (*Engl.Trans.*), 2010, **79**, 945].
3. M. Moniruzzaman, K. I. Winey, *Macromolecules*, 2006, **39**, 5194.
4. P. M. Ajayan, J. M. Tour, *Nature* (*London*), 2007, **447**, 1066.
5. V. G. Udovitsky, *Fiz. Inzh. Poverkhn.*, 2009, **7**, 351 [*Physical Surface Engineering* (*Engl. Transl.*), 2009, **7**, No. 4].
6. L. Vaisman, H. D. Wagner, G. Marom, *Adv. Colloid Interface Sci.*, 2006, **128—130**, 37.
7. O. Tanaike, O. Kimizuka, N. Yoshizawa, K. Yamada, X. Wang, H. Hatori, M. Toyoda, *Electrochem. Commun.*, 2009, **4**, 1441.
8. P. M. Rafailov, C. Thomsen, U. Dettlaff-Weglikowska, S. Roth, *J. Phys. Chem. B*, 2008, **11**, 25368.
9. C. Nieto-Draghi, J. B. Avalosa, *J. Chem. Phys.*, 2003, **119**, 4782.
10. V. V. Chaban, O. N. Kalugin, *J. Mol. Liq.*, 2010, **151**, 113.
11. S. Banerjee, S. S. Wong, *J. Am. Chem. Soc.*, 2002, **124**, 8940.
12. M. Pavese, S. Musso, S. Bianco, M. Giorcelli, N. Pugno, *J. Phys. Condens. Matter*, 2008, **20**, 474206.

13. A. V. Krestinin, A. P. Haritonov, Yu. M. Shulga, O. M. Zhigalina, E. I. Knerelman, M. Dubois, M. M. Brzhezinskaya, A. S. Vinogradov, A. B. Preobrazhencky, G. I. Zvereva, M. B. Kislov, V. M. Martynenko, I. I. Korobov, G. I. Davydova, V. G. Zhigalina, N. A. Kiselev, *Ros. nanotekhnologii*, 2009, **4**, 67 [*Nanotechnologies in Russia* (*Engl. Transl.*), 2009, **4**, 60].
14. A. G. Krivenko, V. I. Matyushenko, E. V. Stenina, L. N. Sviridova, A. V. Krestinin, G. I. Zvereva, V. A. Kurmaz, A. G. Ryabenko, S. N. Dmitriev, V. A. Skuratov, *Electrochem. Commun.*, 2005, **7**, 199.
15. K. Mizur, S. Imafuji, T. Ochi, *J. Phys. Chem. B*, 2000, **104**, 11001.
16. M. C. R. Symons, G. Eaton, *J. Chem. Soc.*, *Faraday Trans. 1*, 1985, **81**, 1963.
17. Yu. A. Kukk, Zh. Klavil´ye, *Elektrokhimiya*, 1977, **13**, 841 [*Sov. Electrochemistry* (*Engl.Trans.*), 1977, **13**, 712].
18. A. P. Dementjeva, K. I. Maslakova, A. V. Naumkin, *Appl. Surf. Sci.*, 2005, **245**, 128.

Received March 4, 2011